

Supplementary Figure Legends

Fig. S1. Amino acid sequence alignment of OST4 from diverse eukaryotes. Sequence alignment of various OST4 homologues was performed with ClustalW2 (<http://www.ebi.ac.uk/Tools/msa/clustalw2/>). Residue conservation values were obtained using Jalview (Waterhouse et al., 2009), and a histogram showing the degree of conservation of each residue is depicted below the sequence alignment. The conservation of residues is shown by shades of grey/yellow; the lighter the colour, the more conserved the residue.

Fig. S2. Comparison of yeast and human OST4 transmembrane regions. (A) Amino acid sequences of human OST4 and *S. cerevisiae* Ost4p. (B) Hydropathy analysis for both human OST4 and *S. cerevisiae* Ost4p was performed using the TMPred program (Hofmann and Stoffel, 1993). Peaks > 500 indicate TM-spanning domains. (C) Prediction of the free energy difference, ΔG_{pred} , for insertion of human OST4 and *S. cerevisiae* Ost4p into the ER membrane was performed using ΔG predictor server (<http://dgpred.cbr.su.se/>) (Hessa et al., 2007). The graphs show predicted ΔG values against position in sequence for different helix lengths ($L = 19\text{--}25$). The more negative the predicted ΔG value of a sequence, the more efficient it can be inserted in the ER membrane. The ΔG_{pred} value after setting residues 10 to 28 of the human OST4 as the TM span (cf. Fig. 1A) is + 0.27, whilst the 19 residue-span of human OST4 with the lowest ΔG_{pred} value (- 0.52) is residues 7 to 25. It should be noted that the lowest ΔG_{pred} value is for the optimal TM span that undergoes ER translocon-mediated membrane integration, and the subsequent assembly of a membrane protein into an oligomeric complex can lead to subsequent alterations in its TM-spanning region (Kauko et al., 2010; Öjemalm et al., 2013).

Fig. S3. Subcellular localisation of exogenously expressed OST4-FLAG in COS-7 cells.

Immunofluorescence microscopy of COS-7 cells expressing either wild-type OST4-FLAG or V23K OST4-FLAG and labelled with the anti-FLAG antibody (red) and an antibody against the ER marker calnexin (green). Scale bars: 10 μm .

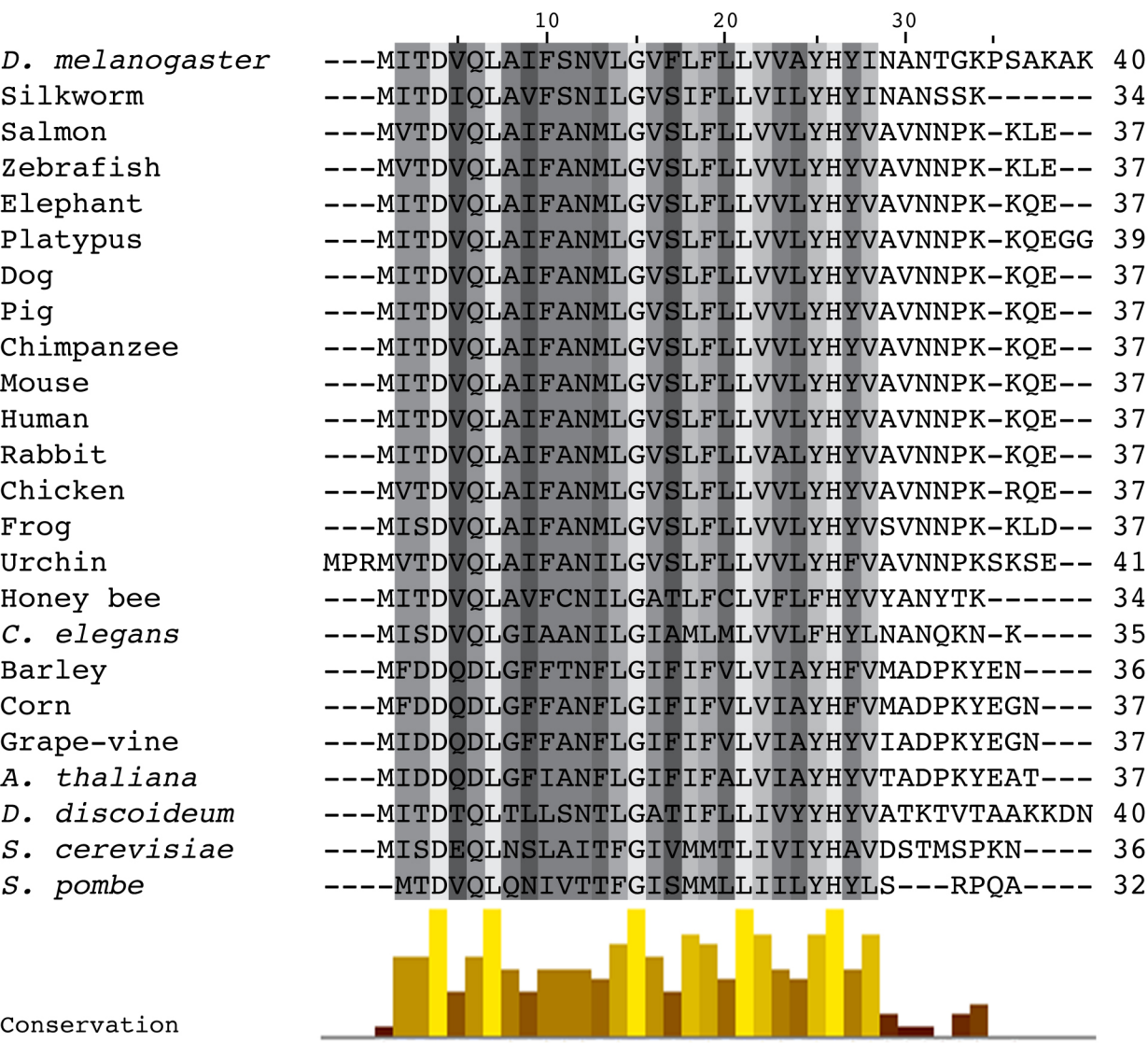
Fig. S4. Depletion of STT3A or ribophorin I destabilises OST4. HeLa cells were transfected with siRNAs targeting STT3A, STT3B, ribophorin I and OST4, or with non-targeting siRNAs (nt, nt₂₇) as a control. Triton X-100-soluble cell extracts were prepared 72 h post-transfection and analysed by immunoblotting with anti-OST4.

Fig. S5. Effect of siRNA-mediated knockdowns on protein levels. The stability and detergent-extractability of OST subunits were analysed by direct solubilisation of siRNA-treated HeLa cells in SDS-PAGE sample buffer, followed by infrared immunoblotting for the proteins indicated. The graph shows the quantification results from this analysis. Fluorescent signals were quantified, normalised to the corresponding γ -tubulin signals, and expressed as a percentage of the signal in control cells.

Fig. S6. Four independent siRNAs targeting OST4 all result in hypoglycosylation of endogenous prosaposin in HeLa cells. HeLa cells were treated with one of four different siRNAs targeting OST mRNA (cf. Figure 4A of main text), or an appropriate control siRNA (nt or nt₂₇), as indicated, and radiolabelled pSAP species were detected by immunoprecipitation and phosphorimaging. The authentically N-glycosylated form of pSAP (pSAP-5), and faster migrating species that lack one or more N-linked glycans (pSAP<5 (xCHO)) are indicated (see also Roboti and High, 2012a).

Fig. S7. siRNA-mediated OST subunit depletion does not induce *XBPI* mRNA splicing. Total RNA was isolated from HeLa cells after 2 h of treatment with 10 mM DTT or after 48 h of transfection with the indicated siRNAs, and *XBPI* mRNA splicing was determined by RT-PCR. Unspliced (*u*) and spliced (*s*) *XBPI* mRNA products are indicated. *GAPDH* served as a loading control.

Figure S1

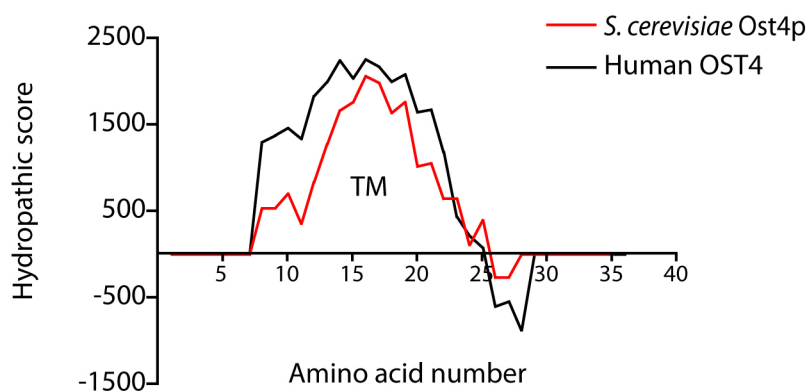


A

A

Human OST4 MITDVQLAIFANMLGVSLFLLVVL¹⁰YHYVA²⁰VNNPKKQE³⁰
S. cerevisiae Ost4p MISDEQLNSLAITFGIVMMTLIV¹⁰IYHA²⁰VDST³⁰MSPKN
 TM

B

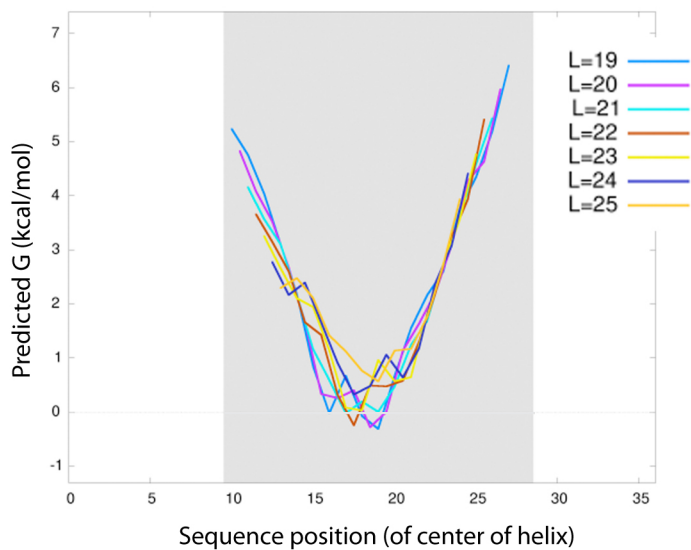


C

S. cerevisiae OST4

Predicted TM helices:

Position	Length	Predicted ΔG	Sequence
10-28	19	-0.315	LAITFGIVMMTLIVIIHAV



Human OST4

Predicted TM helices:

Position	Length	Predicted ΔG	Sequence
7-30	24	-1.157	LAIFANMLGVSLFLLVVLYHYVAV

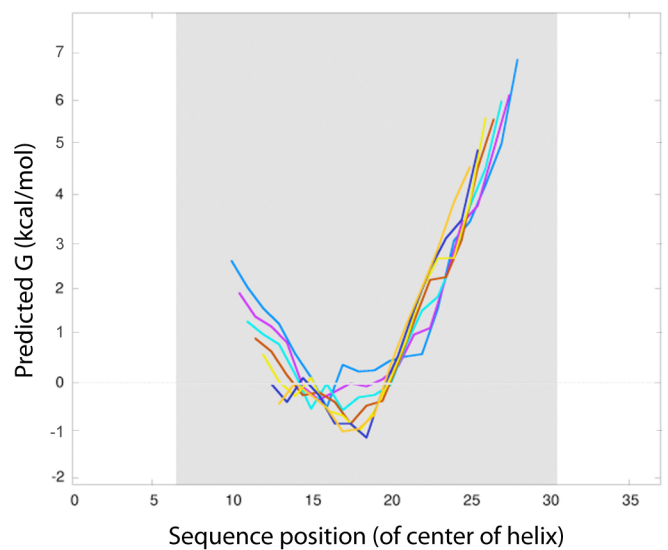


Figure S3

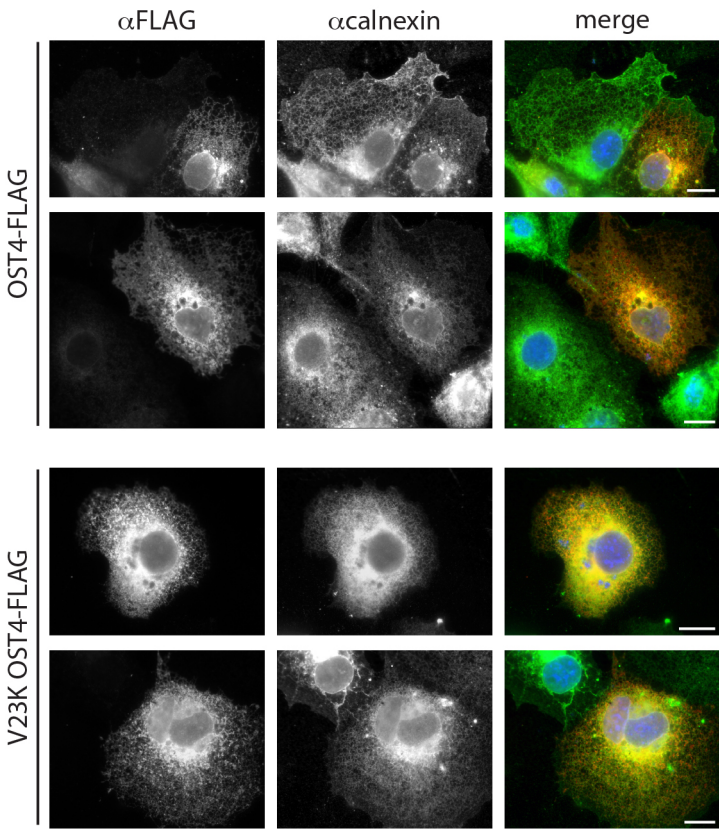


Figure S4

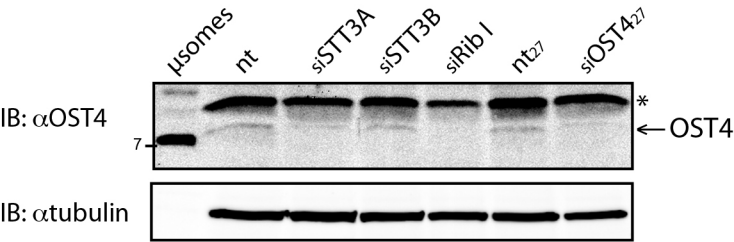
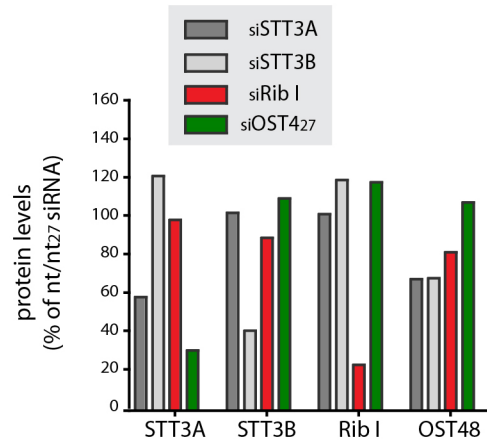
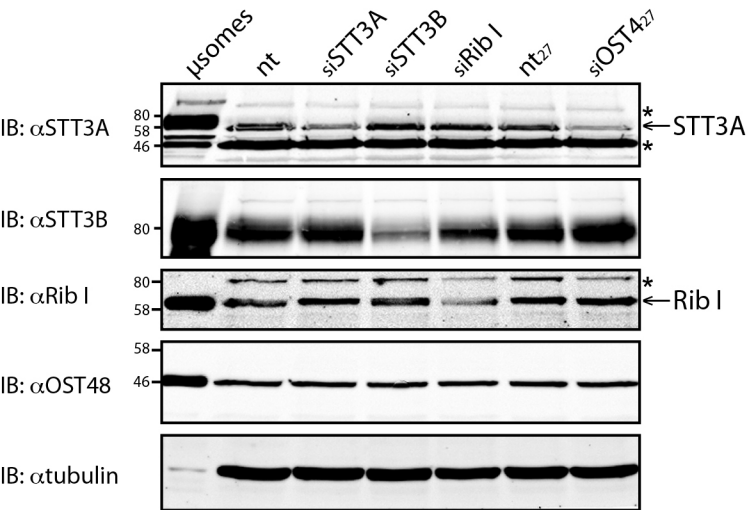


Figure S5



Protein siRNA				
	STT3A	STT3B	Rib I	OST48
siSTT3A	58	102	101	67
siSTT3B	121	40	119	68
siRib I	98	89	22	81
siOST427	30	109	118	107

Figure S6

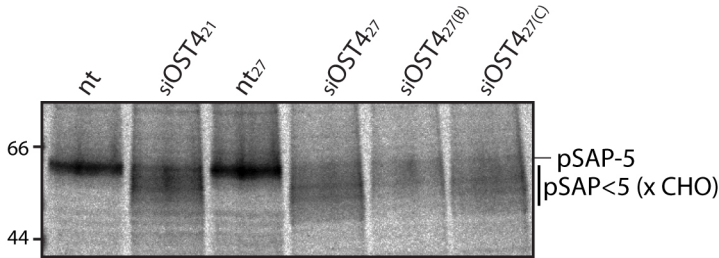


Figure S7

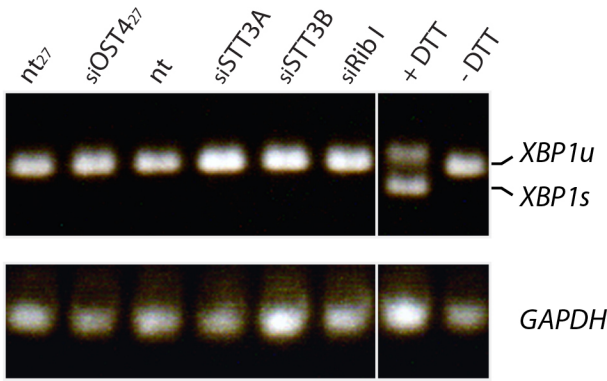


Table S1. The sense strand sequences of siRNAs used in this study

siRNA	Sequence	mRNA / target nucleotides	Source/reference
STT3A	5'-GCGAUUGUCCUAUGAGAAG-3'	STT3A (NM_152713) / 131..149	Ruiz-Canada et al., 2009
STT3B	5'-GCUCUAUAUGCAAUCAGUG-3'	STT3B (NM_178862) / 1330..1348	Ruiz-Canada et al., 2009
Rib I	5'-GCCUUUCACGCUAUGAUdTdT-3'	RPN1 (NM_002950) / 853..871	Ruiz-Canada et al., 2009
OST4 ₂₁	5'-UCACUACGUGGCCGUAACdTdT-3'	OST4 (NM_001134693) / 175..193	this study
OST4 ₂₇	5'-CGUCAACAAUCCCAAGAAGCAGGdAdA-3'	OST4 (NM_001134693) / 187..211	this study
OST4 _{27(B)}	5'-CCCUUCUACCAUACAACAUAACdAdA-3'	OST4 (NM_001134693) / 300..324	this study
OST4 _{27(C)}	5'-CAUAGUCUGAGGCAAGAUGGAGGdGdT-3'	OST4 (NM_001134693) / 248..272	this study

Table S2. Primers used in this study

Primer	Sequence
OST4 For	5'-GACGTGCAGCTCGCCATCTT-3'
OST4 Rev	5'-TGCTTCTTGGGATTGTTGACGGC-3'
Rib I For	5'-CCTATCCAACGAAGACACAAACCA-3'
Rib I Rev	5'-CCATAATCCAGTAGGTCCTCAGAG-3'
Xbp1 For	5'-ACAGCGCTTGGGGATGGATG-3'
Xbp1 Rev	5'-TGA CTGGGTCCAAGTTGTCC-3'
GAPDH For	5'-GGCTGCTTTTAACTCTGGTAAAGT-3'
GAPDH Rev	5'-AACCATGTAGTTGAGGTCATTGAA-3'